An ESR study on electron-capture phosphorus-centered radicals in solid matrixes of alkyl/phenylphosphine sulfides and selenides

Recl. Trav. Chim. Pays-Bas **108**, 262–267 (1989) 0165–0513/89/07/8262–06$2.00

An ESR study on electron-capture phosphorus-centred radicals in solid matrices of alkyl/phenyl phosphine sulfides and selenides

Olav M. Aagaard*, René A. J. Janssen and Henk M. Buck

Department of Organic Chemistry, Eindhoven University of Technology, P.O. Box 513, 5600 MB Eindhoven, The Netherlands
(Received February 17th, 1989)

Abstract. A low-temperature ESR study on electron-capture radicals in X-irradiated alkyl/phenylphosphine chalcogenides is presented. In general, exposure of solid $R_{(3-n)}Ph_nPX$ derivatives (R = alkyl, Ph = phenyl, X = S, Se, $n = 1, 2$) to X-rays gave ESR spectra assigned to the corresponding radical anions, in which the unpaired electron is located in an antibonding P–X σ* orbital. For two of the compounds studied (Me_2PhPSe and $MePh_2PSe$), however, no phosphoranyl radicals could be observed. For methylphenyl-*n*-propylphosphine selenide, a single-crystal ESR analysis of the σ* radical anion is presented, giving detailed information on its electronic and geometric structure. It is found that the unpaired electron resides in a P–Se anti-bonding σ* orbital, whose direction almost parallels the parent P=Se bond. Aspects of radiation damage mechanisms and phosphoranyl radical formation in phosphine chalcogenides are discussed.

Introduction

Over the last decade, the structure of phosphorus-centred radicals has been extensively studied using electron-spin-resonance (ESR) techniques. In particular, the radiogenic formation of phosphorus-centred radicals in single crystals of their precursors has resulted in a detailed description of a number of different radical structures[1]. For four-coordinated phosphorus compounds (R_3PX), X- or γ-irradiation frequently gives rise to an electron-capture reaction, producing a phosphoranyl radical anion. The extra electron can be accommodated in various geometric and electronic configurations[2]. For instance, the radical can adopt a trigonal-bipyramidal (TBP) structure with the odd electron in an equatorial (TBP-e) or axial (TBP-a) location. Alternatively, preserving the original tetrahedral geometry of the parent compound, the unpaired electron can be inserted into the anti-bonding σ* orbital of an existing phosphorus–ligand bond (σ* configuration). Finally, the structural identity can also be intermediate between TBP-e, TBP-a and σ*. The radical configuration which is observed after the irradiation process depends in particular on the nature of the substituents around phosphorus and on the constraints imposed by the surrounding matrix. Recently, we have demonstrated that the stereochemical location of the ligands can also be a decisive factor in the selection of possible configurations[3].

The formation of σ* structures is generally observed upon X-irradiation of four-coordinated phosphorus compounds, in which one bond can accommodate the extra electron more readily than the other three. In agreement with this principle, we were able to identify three-electron σ* radicals

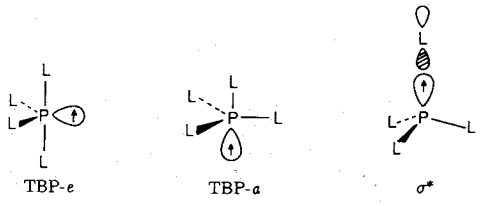

in X-irradiated trialkylphosphine sulfides and selenides (R_3PS and R_3PSe, R = Me, Et, cyclohexyl)[4]. For these radicals, the direction of the singly occupied molecular orbital (SOMO) exactly parallels the parent P=S or P=Se bond, resulting in an axial symmetric configuration. Curiously, X-irradiation of the corresponding triphenylphosphine chalcogenides does not result in electron capture of the phosphorus–chalcogen bond and, in fact, phosphoranyl radicals have never been detected in the pure compounds. The only way to form these species is via irradiation of frozen solutions of the parent compounds in methanol[5] or sulfuric acid[6], where protonation of the sulfur atom is likely to enhance stabilization. Continuing these studies, we wish to present the results of X-irradiation experiments on phosphine sulfides and selenides, in which one or two phenyl groups are present. The introduction of phenyl substituents on phosphorus introduces an additional possible site for electron capture, competing with the P=S or P=Se bond. A second aspect of mixed alkyl/phenyl-substituted phosphine chalcogenides is the fact that the overall geometry of the precursor no longer possesses a three-fold symmetry axis. This, in principle, could lead to structures which deviate more or less from an axial symmetric σ* configuration.

Results

Phenyl-substituted phosphine sulfides

To show the effect of systematic alkyl/phenyl replacements on phosphoranyl radical formation, we studied the radiogenic electron addition of dimethylphenylphosphine sulfide (**1**, Me_2PhPS) and diphenylmethylphosphine sulfide (**2**, $MePh_2PS$).

After a 6-hour exposure to X-rays of a powdered sample of Me_2PhPS (**1**) at 77 K, the ESR spectrum shown in Fig. 1

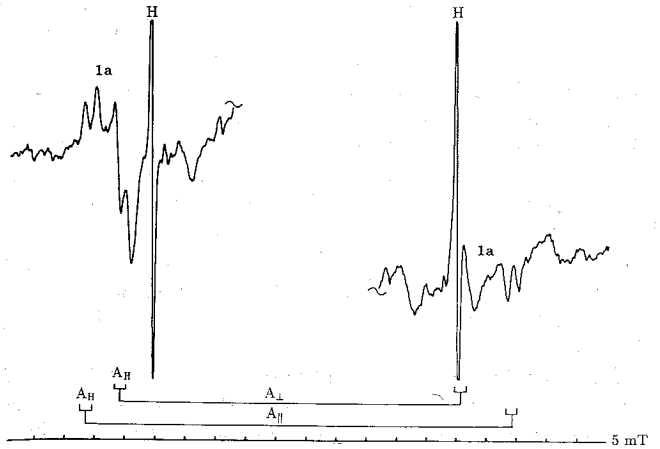

Fig. 1. Powder ESR spectrum of **1a** *at 105 K.*

was recorded. In addition to the intense absorptions of free hydrogen atoms (marked H), the spectrum also reveals the clear parallel ($A_{/\!/}$) and perpendicular ($A_\perp$) hyperfine components of a phosphorus-centred radical (**1a**). In addition to the characteristic large phosphorus hyperfine coupling, a second small and almost isotropic, hyperfine interaction can be observed. The most probable candidate for this second coupling is one of the methyl-hydrogen nuclei. The signal intensity of **1a** is relatively low and its features are irreversibly lost upon raising the temperature to 150 K. No other species was detected on further annealing. The *g* values and hyperfine coupling constants of **1a** were evaluated from the spectrum using the Breit–Rabi equations[7] (Table I).

Given the absence of a significant *g* shift, the isotropic (A_{iso}) and anisotropic or dipolar (A_{dip}) components of the nuclear hyperfine coupling can be obtained from the expressions[7,8]:

$$A_{iso} = (A_{/\!/} + 2A_\perp)/3$$

$$A_{dip} = (A_{/\!/} - A_{iso})/2$$

Using the A_{iso} and A_{dip} components, the valence *s*- and *p*-orbital spin densities can be estimated by comparison with analogous parameters for the free atom[9]. For radical **1a**, this analysis results in $\rho_s = 12.7\%$ and $\rho_p = 35.5\%$ for the central phosphorus nucleus, giving a *p*/*s* ratio of 2.8. The present values of A_{iso} and A_{dip} are almost identical to previous single-crystal ESR data on the σ* trimethylphosphine sulfide radical anion (Table I). We therefore assign **1a** to the dimethylphenylphosphine sulfide radical anion (Me_2PhPS^-) formed via electron addition to the phosphorus–sulfur bond.

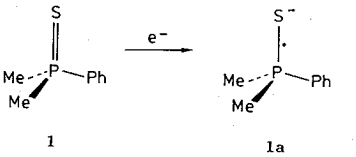

1 1a

The second product which was studied, diphenylmethylphosphine sulfide (Ph_2MePS, **2**), is a viscous oil at room temperature. Rapidly frozen at 77 K to form a clear glassy sample, **2** was X-irradiated for 6 hours. The ESR spectrum recorded at 105 K (Fig. 2a) reveals the presence of the two different phosphorus-centred radicals **2a** and **2b** exhibiting broad resonances. Upon raising the temperature, the signal

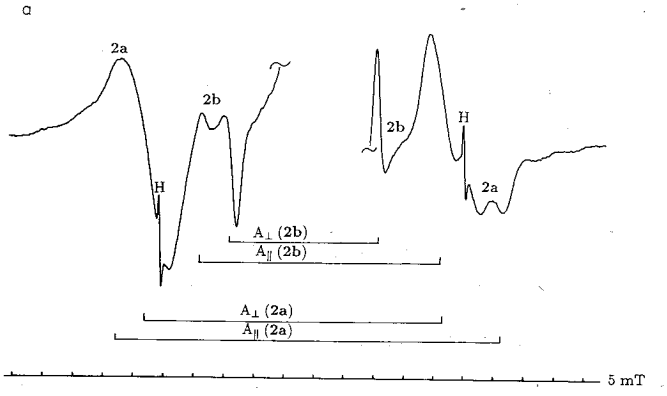

Fig. 2a. Powder ESR spectrum of **2a** *and* **2b** *at 105 K.*

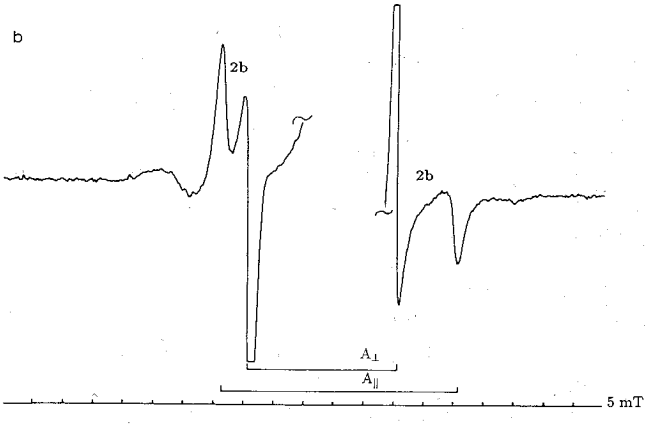

Fig. 2b. Powder ESR spectrum of **2b** *at 225 K.*

Table I Isotropic and dipolar hyperfine couplings, g values and approximate orbital-spin densities.

Radical		A_{iso} (MHz)	$2A_{dip}$ (MHz)	$g_{/\!/}$	$g_\perp$	ρ_s (%)	ρ_p (%)	*p*/*s*
$Me_3\dot{P}S^-$	ref. 4	1776	245	2.003	2.010	13.3	33.3	2.5
Me_2PhPS^-	**1a**	1760	261	2.002	2.007	12.7	35.5	2.8
$MePh_2PS^-$	**2a**	1537	236	2.004	2.015	11.5	32.2	2.8
Ph_3PS^- (CD_3OD)	ref. 5	1485	253			11.1	34.5	3.1
$MePhPrPSe^-$	**5a**	1588	243	1.997	2.057	11.9	33.1	2.8
Ph_2PS	**2b**	831	284	2.003	2.017	6.2	38.7	6.2
Ph_2PS	ref. 10	841	289	2.008	2.017	6.3	39.4	6.2
$MePhPS$	ref. 3	1042	414	1.996	2.012	7.8	56.3	7.2

intensity of the inner doublet **2b** increases at the expense of the outer doublet **2a** (Fig. 2b). At 200 K, radical **2a** is lost. The signals of **2b** persist until the sample melts at 275 K. Radical **2a** is assigned to be a σ* diphenylmethylphosphine sulfide radical anion $MePh_2\dot{P}S^-$. Table I shows that the values of A_{iso} and A_{dip} of **2a** are similar to those of the trimethylphosphine sulfide radical anion[4] and the couplings determined for the triphenylphosphine sulfide radical anion trapped in a γ-irradiated CD_3OD glass[5]. The hyperfine couplings of **2b** are indicative of a phosphonyl type radical ($R_2\dot{P}X$) resulting from a phosphorus–carbon bond dissociation. The estimated spin-density distribution on phosphorus (ρ_s = 6.2% and ρ_p = 38.7%) yields a relatively high *p/s* ratio of 6.2, pointing to a considerable flattening of the original tetrahedral geometry. Comparing the present magnetic parameters with our previous data (Table I) on the diphenylthiophosphonyl radical $Ph_2\dot{P}S$[10,11] and the methylphenylthiophosphonyl radical $MePh\dot{P}S$[3], we assign **2b** to be the $Ph_2\dot{P}S$ species, formed via a dissociation of the P–Me bond.

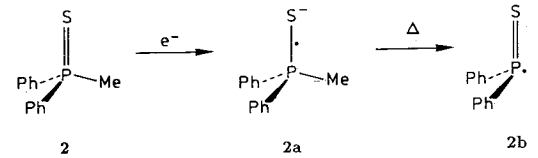

2 **2a** **2b**

The present results show that σ* radical formation is not obstructed by one- or two-fold replacement of a methyl group by a phenyl substituent in phosphine sulfides.

Phenyl-substituted phosphine selenides

X-irradiation of frozen glassy samples of dimethylphenylphosphine selenide (**3**, Me_2PhPSe) and diphenylmethylphosphine selenide (**4**, $MePh_2PSe$) does not result in phosphoranyl radical formation. The ESR spectra of these compounds consist of a broad transition at $g = 2.036$ with no resolvable hyperfine splitting. These signals disappear from the spectra at 200 K. Because of the previously established similarities between X-irradiated phosphine sulfides and selenides[4] the absence of phosphorus-centred radicals is rather surprising. In principle, two different effects can be invoked to rationalize this unexpected result. Firstly, the geometry relaxation, in particular the elongation of the P–Se bond, accompanying the electron-capture process could be prevented in low-temperature rigid matrices, rendering stabilization impossible. Secondly, the orientation of the phenyl ring(s) with respect to the phosphorus chalcogen bond can be favourable for the transfer of the unpaired electron from an initial σ* configuration to the aromatic ring. It is conceivable that the orientation of the phenyl ring influences such a process, since the overlap of the aromatic π orbitals with a P–Se σ* orbital strongly depends on the conformation around the P–Ph bond. The subtle effects governing phosphoranyl radical formation are emphasized by the fact that at least in one case we were able to observe a σ* phosphoranyl radical in a phenyl-substituted phosphine selenide, *viz.* methylphenyl-*n*-propylphosphine selenide (**5**, MePhPrPSe). It is noteworthy that the dihedral angle of the P–Se bond and the phenyl ring of **5**, which can be determined from the reported X-ray crystallographic data[12] amounts to 3.7°, resulting in a small value for the above-mentioned overlap, thereby preventing a secondary reaction of the initial σ* phosphoranyl radical. The R_P and S_P enantiomers of **5** were separately synthesized from the corresponding optically pure phosphines (see Experimental section). Lozenge-shaped crystals of both the R_P and S_P isomer were readily obtained via slow evaporation of cyclohexane solutions. Methylphenyl-*n*-propylphosphine selenide crystallizes in the orthorhombic space group $P2_12_12_1$[12]. The unit cell contains four molecules at the positions (x, y, z), $(\bar{x}, \frac{1}{2}+y, \frac{1}{2}-z)$, $(\frac{1}{2}-x, \bar{y}, \frac{1}{2}+z)$ and $(\frac{1}{2}+x, \frac{1}{2}-y, \bar{z})$. X-irradiation of single crystals of either the R_P or S_P isomer of **5** at 77 K results in the formation of a phosphorus-centred radical (**5a**). The ESR spectrum of a randomly oriented single crystal reveals the presence of four distinct magnetically inequivalent sites, corresponding to the four molecules in the unit cell. For a detailed analysis, the crystals of both R_P- and S_P-**5** were rotated with respect to the magnetic field direction about the three crystallographic axes *a*, *b* and *c* (Fig. 3). Upon rotation of the crystal about any of these axes, the ESR spectrum consists of only two ^{31}P doublets, arising from the coalescence of the four orientations into two pairs (Fig. 4). As would be expected from the crystallographic data, all signals merge into a single ^{31}P doublet when the magnetic field is parallel to any of the axes *a*, *b* or *c*.

Apart from the ^{31}P hyperfine coupling, the high- and low-field transitions are broadened by a poorly resolved ^1H hyperfine coupling, which was estimated to be 25 MHz (0.9–1.0 mT). The signal intensity of the ESR spectra was

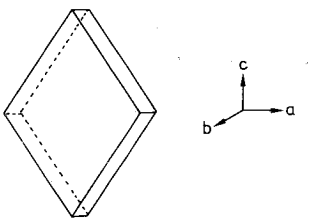

Fig. 3. Schematic drawing of the crystals of **5** *and the ESR reference axes.*

Table II Principal values and direction cosines of the **A** *and* **g** *tensors of* **5a**[a].

Radical	A (MHz)	Direction cosines			g	Direction cosines		
		a	*b*	*c*		*a*	*b*	*c*
R_P	A_1 1454	0.611	0.455	−0.647	g_1 1.996	0.138	0.415	0.899
	A_2 1474	0.692	−0.704	0.158	g_2 2.001	0.404	0.805	−0.434
	A_3 1834	0.383	0.544	0.746	g_3 2.055	−0.905	0.423	−0.057
S_P	A_1 1461	0.753	0.264	−0.603	g_1 1.997	0.235	0.625	0.744
	A_2 1479	0.533	−0.782	0.323	g_2 2.002	0.333	0.667	−0.666
	A_3 1827	0.386	0.565	0.729	g_3 2.057	−0.913	0.405	−0.051

[a] The direction cosines are listed for one of the four possible sites. The remaining three orientations are related to (x, y, z) by $(x, -y, -z)$, $(-x, y, -z)$ and $(-x, -y, z)$.

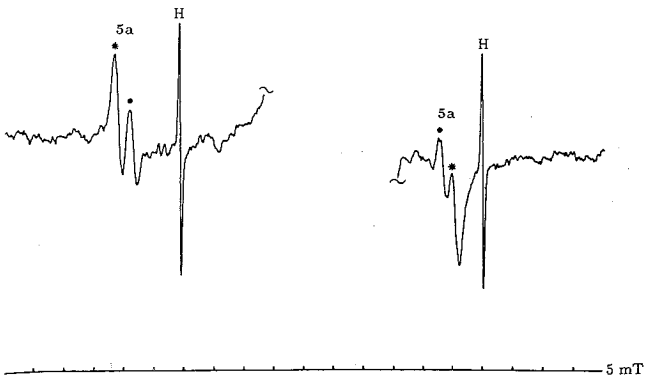

Fig. 4. Single-crystal ESR spectrum of **5a** *at 105 K.*

too weak to allow an analysis of the ^{77}Se satellite splittings (^{77}Se isotope, $I = \frac{1}{2}$, natural abundance 7.53%).

The ESR spectra of **5a** were analysed using the following Hamiltonian:

$$H = \beta \boldsymbol{S} \cdot \boldsymbol{g} \cdot \boldsymbol{B} - g_N \beta_N \boldsymbol{I} \cdot \boldsymbol{B} + \boldsymbol{S} \cdot \boldsymbol{A} \cdot \boldsymbol{I}$$

where all symbols have their usual definition and $\boldsymbol{A}$ describes the ^{31}P hyperfine interaction. In order to obtain an accurate determination of the magnetic parameters $\boldsymbol{A}$ and $\boldsymbol{g}$, the observed field positions were used in a least-squares routine producing an analytical expression for the orientational dependence of the ESR transitions. The $\boldsymbol{g}$ and $\boldsymbol{A}$ tensors were initially estimated using second-order perturbation theory and subsequently optimized in an iterative routine to reproduce the observed field positions for a number of special orientations (*i.e.* where the magnetic field parallels or bisects the crystallographic axes). The last step consisted of an accuracy test of the final $\boldsymbol{g}$ and $\boldsymbol{A}$ tensors (Table II). The observed (B_{obs}) and calculated field values (B_{calc}), obtained via exact diagonalization of the Hamiltonian, were compared (Fig. 5) and the value of the rms error (ΔB) was determined.

$$\Delta B = \left[\left[\sum_i^n [B_{obs}(i) - B_{calc}(i)]^2 \right] / n \right]^{1/2}$$

For the present single-crystal ESR studies, this value was less than 0.2 mT, *i.e.* approximately a tenth of the line width.

Table II indicates that the radicals formed in both the R_P and S_P isomer are virtually identical and allow a check of the overall accuracy of the single-crystal analysis to be made. In this respect, it should be noted that, for two (almost) degenerate eigenvalues, the corresponding eigenvectors cannot be very accurate. This explains the differences between the direction cosines of A_1, A_2, g_1 and g_2 for the R_P and S_P components. The A_{iso} and A_{dip} (Table I) components can be derived from the three principal values[7]:

$$A_{iso} = (A_1 + A_2 + A_3)/3$$

$$A_{dip} = (A_3 - A_{iso})/2$$

Subsequently, the valence orbital spin densities are obtained in the usual way, resulting in $\rho_s = 11.8\%$ and $\rho_p = 31.8\%$,

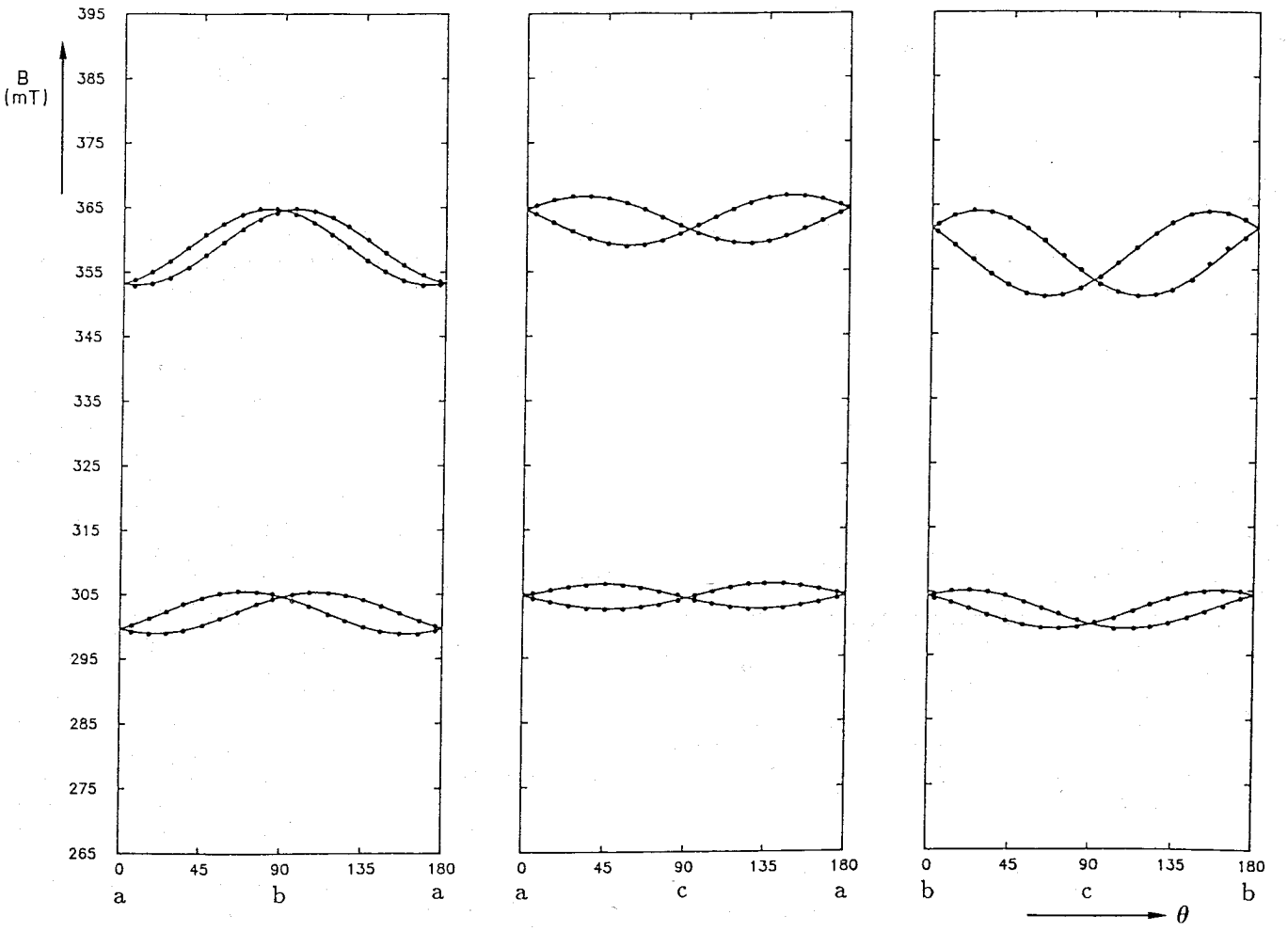

Fig. 5. Angular dependence of the low- and high-field ESR transitions of **5a**.

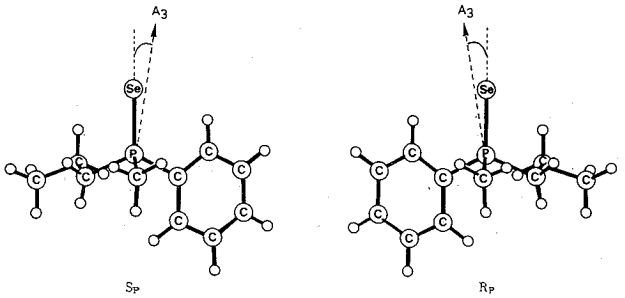

*Fig. 6. Direction of the SOMO for S_P- and R_P-**5a**.*

giving a *p/s* ratio of 2.7. In addition, the single-crystal analysis affords the direction of the largest phosphorus hyperfine coupling, which corresponds to the direction of the SOMO. It is found that the SOMO is not exactly aligned with the parent P=Se bond, but that there is a small angle (8–9°) between them. Table III compiles all angles of the SOMO of R_P- and S_P-**5a** with the four phosphorus–ligand bonds.

Table III Angles of the SOMO of **5a** *with respect to the four phosphorus ligand bonds.*

Angle	X = Se	X = SOMO	
		R_P	S_P
X–P–Se	0	8.6	8.7
X–P–Ph	113.8	106.2	105.5
X–P–Me	112.9	120.2	119.4
X–P–Pr	112.6	112.6	114.1

To facilitate comparison, the angles between the P=Se bond and the remaining three bonds are included. It can be seen that the SOMO points more or less towards the phenyl substituent and away from the methyl group (Fig. 6). All structural data lead to the conclusion that both isomers of **5a** possess a three-electron P–Se bond in which the unpaired electron is located in the antibonding σ* orbital.

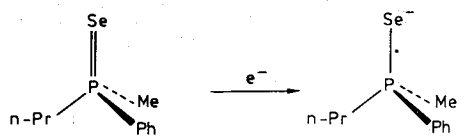

Discussion

The present results show that, in principle, the generation of σ* phosphoranyl radicals is not obstructed by single or double replacement of an alkyl group by a phenyl group in chalcogeno phosphines. The A_{iso} and A_{dip} couplings for the σ* radicals **1a**, **2a**, **5a** are similar to those found for other σ* chalcogeno trialkylphosphine radical anions, thus supporting the assignments. Table I shows that an increase in the number of phenyl substituents results in a steady decrease of A_{iso}, and thus of ρ_s. For the diphenylmethylphosphine sulfide (**2**), a secondary radical **2b** is observed on warming. Based on the concurrent loss of **2a**, **2b** seems to originate from the σ* radical anion. The most probable candidate for this species is the diphenylthiophosphonyl radical, formed by a cleavage of the P–Me bond. Several mechanisms can explain the formation of **2b**. X-irradiation of solid diphenylmethylphosphine sulfide results, after initial ionization (1), in electron capture (2):

$$MePh_2PS \rightarrow [MePh_2\dot{P}S]^+ + e^- \quad (1)$$

$$MePh_2PS + e^- \rightarrow [MePh_2\dot{P}-S]^- \quad (2)$$

These two reactions can be followed on annealing by processes (3), (4) or (5) resulting in the formation of **2b**.

$$[MePh_2\dot{P}-S]^- + [MePh_2\dot{P}S]^+ \rightarrow MePh_2PS^* + MePh_2PS \quad (3a)$$

$$MePh_2PS^* \rightarrow Ph_2\dot{P}S + \dot{M}e \quad (3b)$$

or

$$[MePh_2\dot{P}-S]^- \rightarrow [Ph_2P(S)^{\bullet}Me]^{-\neq} \rightarrow Ph_2\dot{P}S + Me^- \quad (4)$$

or

$$[MePh_2\dot{P}S]^+ \rightarrow Ph_2\dot{P}S + Me^+ \quad (5)$$

The actual route by which **2b** is formed cannot be unambiguously determined. Reaction (3) postulates charge recombination, leading to an electronically and vibrationally excited molecule which subsequently undergoes homolytic bond fission. Reaction (4) involves a thermal transition state with a σ* P–Me bond.

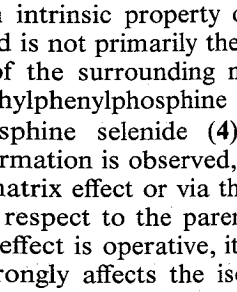

The elongation of this linkage, induced by the anti-bonding character, results in the observed dissociation. Reaction (5) explains the formation of **2b**, but would imply that the simultaneous loss of **2a** is coincidental. We suggest process (4) to be the most probable, since formation of methyl radicals as in (3) is not observed and reaction (5) does not involve the anionic species **2a**.

The single-crystal analysis of the R_P and S_P enantiomers of **5** shows that the SOMO almost parallels the P=Se bond. This indicates that the formation of an axial symmetric σ* configuration is an intrinsic property of the phosphorus–chalcogen bond and is not primarily the result of a C_3-symmetry constraint of the surrounding matrix. The present results on dimethylphenylphosphine selenide (**3**) and diphenylmethylphosphine selenide (**4**), where no phosphoranyl radical formation is observed, can be rationalized on the basis of a matrix effect or via the orientation of the phenyl group with respect to the parent P–Se bond (*vide supra*). If a matrix effect is operative, it would be expected that the matrix strongly affects the isotropic and dipolar hyperfine couplings. However, the magnetic parameters of radicals **1a**, **2a** and **5a** are in good agreement with other σ* species (Table I) and a continuous decrease of A_{iso} is established for progressive phenyl substitution. Similar trends were obtained in the series of σ* trimethyl-, triethyl- and tricyclohexylphosphine chalcogenide radical anions[4]. At present, there are insufficient data available to support the suggestion that the orientation of the aromatic ring determines the formation of phosphoranyl radicals in phenyl-substituted phosphine chalcogenides. The formation of **5a**, however, is in excellent agreement with this principle.

We therefore suggest that the electronic structure of a phosphoranyl radical, resulting from low-temperature solid state X-irradiation, is primarily a consequence of the intrinsic properties of the isolated parent molecule.

Experimental

ESR

ESR measurements were performed using a Bruker ER 200D spectrometer, operating with an X-band standard cavity. The spectra were recorded digitally using a Bruker Aspect 3000 computer. In a typical run, a sweep of 187.5 mT was sampled with 4 K data points, resulting in a resolution of 0.045 mT. Microwave power was 2 mW in most experiments. Crystals were rotated about an axis perpendicular to the magnetic field from 0 to 180°, in 10° steps, with a single-axis goniometer. Temperature was controlled with the aid of a variable temperature unit.

X-irradiation

The compounds were X-irradiated in sealed quartz tubes in a glass Dewar vessel containing liquid nitrogen (77 K) with unfiltered radiation from a Cu anticathode operating at 40 kV and 20 mA.

Synthesis

All experiments were carried out under an atmosphere of dry nitrogen. Solvents were dried by standard methods. NMR spectra were recorded on a Bruker AC 200 spectrometer; chemical shifts are reported relative to TMS (^{1}H) or 85% H_3PO_4 (^{31}P, external standard) and downfield shift are quoted positive.

Phosphine sulfides and selenides **1–4**. *General procedure*

Equimolar amounts of elemental sulfur or selenium and phosphine were reacted in dry toluene. Subsequently, the solvent was removed and the products were obtained in almost pure form and quantitative yields[13].

Dimethylphenylphosphine sulfide (**1**)

White crystals, m.p. 46°C, b.p. 90°C (0.12 mmHg). ^{1}H NMR ($CDCl_3$): δ 1.99 (d, 6H, CH_3, J_{PCH} 13.2 Hz), 7.53 (m, 3H, *m*-PhH and *p*-PhH), 7.92 (m, 2H, *o*-PhH). ^{31}P NMR ($CDCl_3$): δ 33.3.

Diphenylmethylphosphine sulfide (**2**)

Clear viscous liquid, b.p. 142–146°C (0.08 mmHg). ^{1}H NMR ($CDCl_3$): δ 2.28 (d, 3H, CH_3, J_{PCH} 13.2 Hz), 7.48 (m, 6H, *m*-PhH and *p*-PhH), 7.83 (m, 4H, *o*-PhH). ^{31}P NMR ($CDCl_3$): δ 36.5.

Dimethylphenylphosphine selenide (**3**)

Yellowish oil. ^{1}H NMR ($CDCl_3$): δ 2.18 (d, 6H, CH_3, J_{PCH} 13.2 Hz), 7.50 (m, 3H, *m*-PhH and *p*-PhH), 7.93 (m, 2H, *o*-PhH). ^{31}P NMR ($CDCl_3$): δ 16.6, J_{PSe} 703 Hz.

Diphenylmethylphosphine selenide (**4**)

Yellowish oil. ^{1}H NMR ($CDCl_3$): δ 2.47 (d, 3H, CH_3, J_{PCH} 13.2 Hz), 7.54 (m, 6H, *m*-PhH and *p*-PhH), 7.82 (m, 4H, *o*-PhH). ^{31}P NMR ($CDCl_3$): δ 23.8, J_{PSe} 718 Hz.

Methylphenyl-n-propylphosphine selenide (**5**)

The optically pure R_P and S_P phosphines were synthesized according to the procedure outlined by *Mislow* et al.[14,15] from the *d*- and *l*-menthylmethylphenylphosphinates, respectively. After several crystallizations from α-(−)-pinene, the diastereoisomerically pure phosphinates were obtained. Reaction of the phosphinates with *n*-propylmagnesium bromide affords the optically pure methylphenyl-*n*-propylphosphine oxides, which can be deoxygenated stereospecifically using hexachlorodisilane. The last step consists of reaction with elemental selenium[16]. The products were crystallized several times from cyclohexane. Circular dichroism: R_P negative Cotton effect, S_P positive Cotton effect, both at 270 nm. ^{1}H NMR ($CDCl_3$): δ 1.00 (dt, 3H, CCH_3), 1.62 (m, 2H, CCH_2C), 2.15 (d, 3H, PCH_3, J_{PCH} 13.0 Hz), 2.17 (m, 2H, PCH_2), 7.52 (m, 3H, *m*-PhH and *p*-PhH), 7.92 (m, 2H, *o*-PhH); ^{31}P NMR ($CDCl_3$): δ 26.6, J_{PSe} 706 Hz.

Acknowledgement

This investigation was supported by the Netherlands Foundation for Chemical Research (SON) with financial aid from the Netherlands Organization for Scientific Research (NWO).

References and Notes

1 For a recent compilation of data see *P. Tordo*, "Landolt–Börnstein, New Series", Volume II 17/e, p. 254, Springer-Verlag, Berlin, 1988, and references cited therein.
2 *W. G. Bentrude*, Acc. Chem. Res. **15**, 117 (1982).
3 *R. A. J. Janssen, M. J. van der Woerd, O. M. Aagaard* and *H. M. Buck*, J. Am. Chem. Soc. **110**, 6001 (1988).
4 *R. A. J. Janssen, J. A. J. M. Kingma* and *H. M. Buck*, J. Am. Chem. Soc. **110**, 3018 (1988).
5 *J. C. Evans* and *S. P. Mishra*, Chem. Phys. Lett. **72**, 168 (1980).
6 *S. P. Mishra* and *M. C. R. Symons*, J. Chem. Soc. Perkin Trans. II 21 (1976).
7 *W. Weltner*, "Magnetic Atoms and Molecules", Scientific and Academic Editions, New York, 1983.
8 The three principal values of the nuclear hyperfine coupling tensor of an axial symmetric radical are given by $A_1 = A_\perp = A_{iso} - A_{dip}$, $A_2 = A_\perp = A_{iso} - A_{dip}$, and $A_3 = A_{/\!/} = A_{iso} + 2A_{dip}$, where A_{iso} and A_{dip} are the isotropic and dipolar (or anisotropic) hyperfine coupling constants. See ref. 7, page 55.
9 *J. R. Morton* and *K. F. Preston*, J. Magn. Reson. **30**, 577 (1978).
10 *R. A. J. Janssen, M. H. W. Sonnemans* and *H. M. Buck*, J. Chem. Phys. **84**, 3694 (1986).
11 The A_{iso} and A_{dip} values of Ph_2PS reported by *M. Geoffroy*, Helv. Chim. Acta **56**, 1552 (1973), in a single-crystal analysis are somewhat larger (A_{iso} = 994, A_{dip} = 328 MHz). This difference may result from the proximity of the dissociated fragment, *i.e.* H or Me.
12 *Z. Galdecki, M. L. Glowka, J. Michalski, A. Okruszek* and *W. J. Stec*, Acta Cryst. Sect. B. **33**, 2322 (1977).
13 *P. Haake, R. D. Cook* and *G. H. Hurst*, J. Am. Chem. Soc. **89**, 2650 (1967).
14 *O. Korpiun, R. A. Lewis, J. Chickos* and *K. Mislow*, J. Am. Chem. Soc. **90**, 4842 (1968).
15 *K. Naumann, G. Zon* and *K. Mislow*, J. Am. Chem. Soc. **91**, 7012 (1969).
16 *W. J. Stec, A. Okruszek* and *J. Michalski*, Angew. Chem. **83**, 491 (1971).